



Synthesis and characterization of La- and Ce-codoped polycrystal ZnO prepared by hydrothermal method for 1,2-propanediol

Wenrui Lu¹ · Dachuan Zhu¹

Received: 23 October 2018 / Accepted: 2 January 2019 / Published online: 4 January 2019
© Springer-Verlag GmbH Germany, part of Springer Nature 2019

Abstract

La/Ce-codoped ZnO (La/Ce–ZnO)-based gas sensors are successfully prepared by a simple mild hydrothermal method. And the structures, morphologies and sensing properties are examined by XRD, SEM and XPS, respectively. The 1,2-propanediol gas-sensing analysis reveals that the La/Ce–ZnO-based gas sensor displays the highest response compared with La-doped ZnO and Ce-doped ZnO sensors. La/Ce–ZnO-based gas sensor exhibits an excellent response (681) and possesses good response and recovery property of 11 and 45 s to 100 ppm 1,2-propanediol at 240 °C, respectively. The mechanism of gas sensing and enhanced gas response of La/Ce–ZnO is discussed.

1 Introduction

Semiconductors doped with rare earth (RE) ions have attracted much attention and are promising for use in gas sensors. Several researchers have found that rare earth ions have outstanding properties, such as increasing the amount of active sites and excellent catalytic properties [1, 2]. For these reasons, the method of doping RE ions in oxide semiconductors, such as ZnO, SnO₂, and WO₃, has gained a great deal of interest [3, 4]. Among these oxide semiconductors, zinc oxide (ZnO), an important member in the II–IV groups, finds applications in the field of piezoelectric, optoelectronic and solar cell [2, 5, 6]. We synthesize La-doped ZnO, Ce-doped ZnO and La/Ce–ZnO samples by hydrothermal method. In addition, ZnO has been considered as a promising material for gas sensors because of its chemical sensitivity to volatile and other toxic gases, suitability to be doped, non-toxicity, abundance in nature and low cost [7, 8]. Unfortunately, ZnO usually performs outstanding gas-sensing properties only at very high temperature (> 300 °C) which will cause energy consumption and deteriorate the stability of gas sensor [9]. So, it is quite necessary to lower the operating temperature without sacrificing other gas-sensing properties such as sensor response, repeatability and stability

[10, 11]. Especially, incorporation of lanthanides into ZnO has been proved as a feasible way to realize the tailoring of the band gap through a change in the charge carrier concentration. Usually, these rare earth elements are used as catalyst in the form of oxides or oxysalts decorated on the ZnO surface. For example, La₂O₃ can offer new opportunities for enhancing the gas-sensing performance based on semiconducting oxides owing to its high thermal stability and strong surface basicity [2]. CeO₂, as one of important rare earth oxides, has received remarkable attention due to its wide application in catalysis. Owing to its outstanding oxygen storage capacity, CeO₂ exhibits an excellent effect on the reactivity of the catalysts [12]. The process of using RE ions as activator and semiconductors as host combines the advantage of the gas-sensing properties of RE ions and the unique properties of the semiconductors.

Based on previous work of our laboratory, we found that 3 at.% Ce-doped ZnO sensor exhibited a maximum sensitivity for 1,2-propanediol at the optimum operating temperature [13], so we choose different systems with a total dopant concentration of 3 at.% (3 at.% CeO₂/3 at.% La₂O₃/1.5 at.% CeO₂ + 1.5 at.% La₂O₃) in this paper to investigate the coordination effect on the gas-sensing properties between CeO₂ and La₂O₃. Meanwhile, their microstructure and sensing mechanism are investigated. In addition, the sensing sensitivities, including gas response, short- and long-term stability and selectivity, of different samples have been studied.

✉ Dachuan Zhu
zhudachuan@scu.edu.cn

¹ College of Material Science and Engineering,
Sichuan University, Chengdu 610065, Sichuan,
People's Republic of China

2 Experimental

2.1 Preparation

All the reagents used in the experiment are of analytical grade and used without further purification. La/Ce-doped ZnO samples are prepared via hydrothermal method. In a typical procedure, 10 mL NaOH (2 mol/L) solution is added slowly to a constantly magnetically stirred mixture containing 0.439 g $\text{Zn}(\text{CH}_3\text{COO})_2 \cdot 2\text{H}_2\text{O}$, 0.2 g PEG with designed atomic ratio of $\text{Ce}(\text{NO}_3)_3 \cdot 6\text{H}_2\text{O}$, and $\text{La}(\text{NO}_3)_3 \cdot 6\text{H}_2\text{O}$ at room temperature for 0.5 h. After vigorous stirring, the solution is finally transferred into a Teflon-lined autoclave (50 mL) and kept at 150 °C for 12 h. The pale white product is formed and washed with DI water and ethanol several times to remove by-products. The product is dried at 80 °C for 8 h, finally followed by calcination in air at 500 °C for 1 h. White powder is finally obtained.

2.2 Characterization

The crystal phases of as-prepared materials are characterized by XRD (XRD-6000, SHIMADZU). The morphology of the synthesized samples is examined by SEM (JEOL JSM-5900LV, Japan) and EDS technique is applied to determine their elemental compositions. The prepared process of samples for SEM in detail is listed as following: the doped ZnO powder is dispersed by ultrasonic in ethyl alcohol solution for 5 min, then dripped on a silicon plate. After the dispersed ZnO powders are dried, Au powders are sprayed on their surface to improve the electric conductivity of the doped ZnO sample. XPS (XSAM800) is used to assess the chemical state.

2.3 Fabrication and measurement of gas sensor

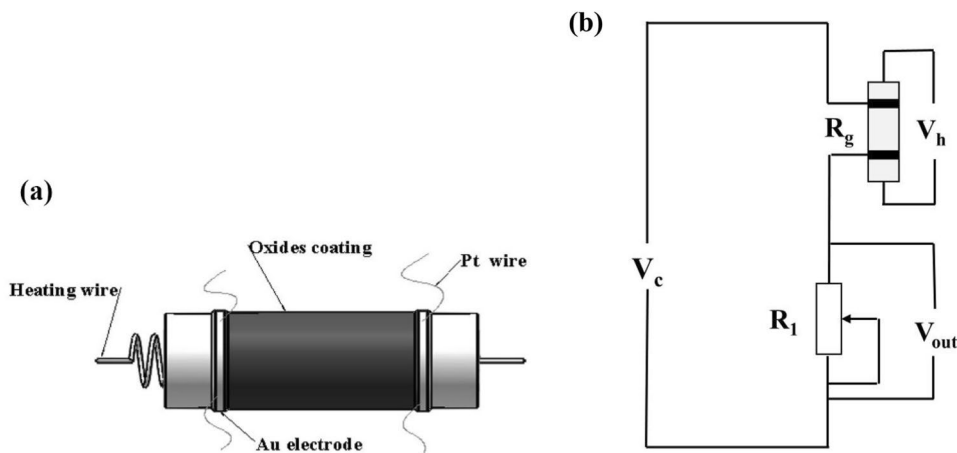
An appropriate amount of the as-prepared ZnO is mixed with anhydrous ethanol, and then ultrasonic dispersed until it becomes homogeneous. Then the paste is coated onto Al_2O_3 ceramic tube connecting with two Au electrodes and a pair of platinum wires at both bottoms (Fig. 1a). Then the tube is calcined at 500 °C for 1 h. Subsequently, a heater of Ni–Cr wire ($R \approx 22\Omega$) is inserted into the ceramic tube to regulate the operating temperature. Finally, the sensor sample is soldered onto the bakelite base via by the platinum wires. To increase their stability, the fabricated sensors are aged for 5 days in air. The WS-30B system (Weisheng Instrument Co., Zhengzhou, China) is used to measure the gas-sensing performance of these sensors. The schematic of the basic measuring electric circuit is shown in Fig. 1b. The sensor response is defined as $S = R_a/R_g$, where R_a and R_g denote the resistance of the sensor exposed to clean air and to reductive gas, respectively.

3 Results and discussion

3.1 Characterization of microstructure

Figure 2 shows the XRD patterns of the as-prepared ZnO samples. It can be clearly observed that the diffraction peaks of the sample can be readily indexed to the hexagonal wurtzite ZnO phase, which is very well matched with the standard data (JCPDS card no. 36-1451). Besides, weaker diffraction peaks located at 28.6° and 29.0° can be indexed to (111), (011) planes belonging to cubic structure CeO_2 (JCPDS no. 78-0694) and La_2O_3 (JCPDS no. 83-1345), respectively (see Fig. 2b). Hence, in case of the valency of Ce^{3+} in the cerium nitrate hexahydrate, there is a variation of valency after

Fig. 1 Schematic illustration of the gas sensor (a) and the electrical circuit for the gas-sensing test (b) (V_h heating voltage, V_c circuit voltage, V_{out} signal voltage, R_l load resistor)



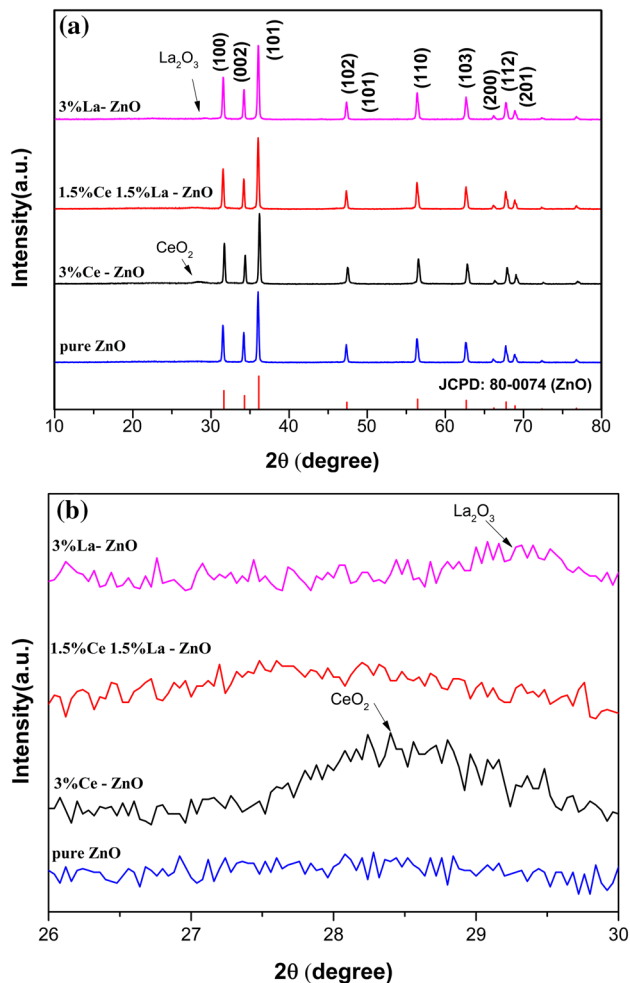


Fig. 2 XRD patterns of pure ZnO, La-doped ZnO, Ce-doped ZnO and La/Ce-codoped ZnO (a) and magnification in 26.5°–30° (b)

Table 1 The lattice constants calculated from XRD

ZnO	Lattice constants a (Å)	Lattice constants c (Å)	Vol
ZnO (no. 80-0074)	3.2498	5.2066	142.8587
La-doped ZnO	3.2541	5.2101	143.3333
La/Ce-codoped ZnO	3.2580	5.2131	143.7598
Ce-doped ZnO	3.2557	5.2096	143.4605

calcinations of the samples. In addition, it can be seen that the (002) diffraction peak slightly shifts to a lower degree due to the incorporation of partial La and/or Ce into ZnO lattice. What's more, no trace of any other compounds such as $\text{Zn}(\text{OH})_2$ and ZnO_2 can be found in the diffraction patterns, indicating that the samples consist of three separated phases of ZnO, La_2O_3 and CeO_2 . Table 1 gives the lattice constant and cell volume calculated from XRD. It can be seen that the

lattice parameters and cell volume of La/Ce-codoped ZnO are bigger than those of La-doped ZnO and Ce-doped ZnO.

To examine the morphologies, the as-prepared ZnO samples are characterized by scanning electron microscopy (SEM). As can be seen from the Fig. 3, the typical length and average diameter of each ZnO rods are in the range of 2–5 μm and 100–200 nm, respectively. And some ZnO rods are assembled into non-homogeneously distributed flower-shaped structure. The average diameter of each flower structure is 8–10 μm . Owing to the doped particle congregating on the surface of the ZnO rods, the surface of ZnO rods becomes coarsened.

Elemental composition and purity of La/Ce-codoped ZnO is conducted on EDX. As shown in the prepared process of samples for SEM, the area of the silicon plate is much larger than that of the doped ZnO sample and Au powders cover all the surfaces as a thin layer, so Si and Au are detected additionally. Meanwhile, Si-related peak in Fig. 3f is many times higher than that of Zn, La, and Ce. The result shown in Fig. 3f confirms that apart from Si and Au caused by the detection process, La/Ce-codoped ZnO is mainly composed of zinc, oxygen, cerium and lanthanum. Thus, this La/Ce-codoped ZnO is highly pure without any impurities or contaminations.

To further confirm the chemical composition of the La/Ce-codoped ZnO, the XPS studies are carried out. As we can observe in Fig. 4, there are no extra peaks corresponding to any impurities except Zn, O, C, La and Ce, indicating the high purity of La/Ce-codoped ZnO. The Zn 2p spectra show symmetric peaks which are centered at 1021.6 and 1044.7 eV correspond to Zn 2p_{3/2} and Zn 2p_{1/2}, respectively. From the O 1s spectrum shown in Fig. 4b, the peak centered at 530.3 eV is attributed to O^{2-} ions in ZnO, while the peak located at 532.1 eV is assigned to the hydroxyl species on the catalyst surface. As is known to all, there are two different oxidation states for the element Ce. But, in the Ce 3d spectrum, the peaks positioned at 880.0, 895.8, and 914.1 eV are assigned to the characteristic peaks of Ce^{4+} . The La 3d spectrum has four peaks at 835.1, 838.6, 851.9 and 854.6 eV which indicated that La is present in La/Ce-codoped ZnO sample in the form of La^{3+} .

3.2 Measurement of gas-sensing properties

It is well known that the response of a semiconductor gas sensor is greatly influenced by the operating temperature. Figure 5 shows the sensitivity–temperature curve of the ZnO to 100 ppm 1,2-propanediol at the operating temperatures in range of 200–340 °C. It can be seen that each sample has only one optimal operating temperature. Obviously, when compared with singly La-doped ZnO or Ce-doped ZnO sensors, the sensor based on La/Ce-codoped ZnO exhibits maximum sensitivity at a lower operating temperature of 240 °C,

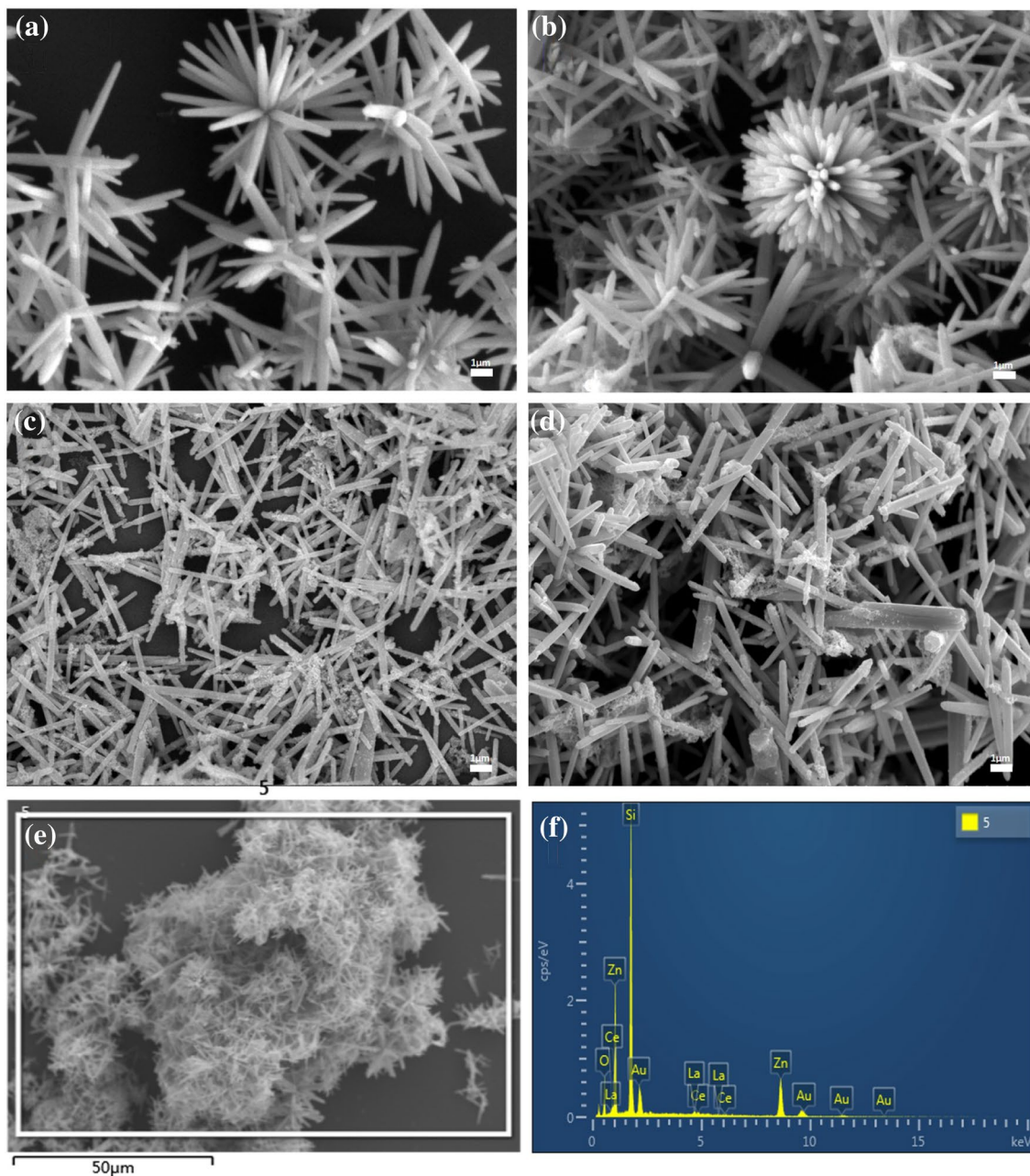


Fig. 3 SEM images of pure ZnO (a), 3 at.% La-ZnO (b), 1.5 at.% La/1.5 at.% Ce-ZnO (c), 3 at.% Ce-ZnO (d), EDS analysis of La/Ce-ZnO (e, f)

especially with remarkably increased response of 681 which is about three times higher than that of La-doped ZnO- and Ce-doped ZnO-based sensors to 100 ppm 1,2-propanediol at 240 °C. So, 240 °C is chosen as the optimum operating temperature.

Figure 6 displays the dynamic response–recovery curve of La/Ce-codoped ZnO-based gas sensor when it is orderly exposed to 1,2-propanediol atmosphere ranging from 1 to 400 ppm at 240 °C. These results are observed to be repeatable of all concentrations of 1,2-propanediol. The

corresponding responses of the sensor are highly dependent on the concentration of 1,2-propanediol, and Fig. 7 shows an approximately linear increasing trend in the range of 1–100 ppm. The linear correlation coefficient is 0.988. But once the concentration surpasses 200 ppm, the sensitivity increases slowly, even inconspicuously. The result indicates that the concentration of the adsorbed oxygen tends to be saturated on the limited adsorption sites.

Figure 8 shows a typical response and recovery curve of the three sensors when they are exposed to 100 ppm

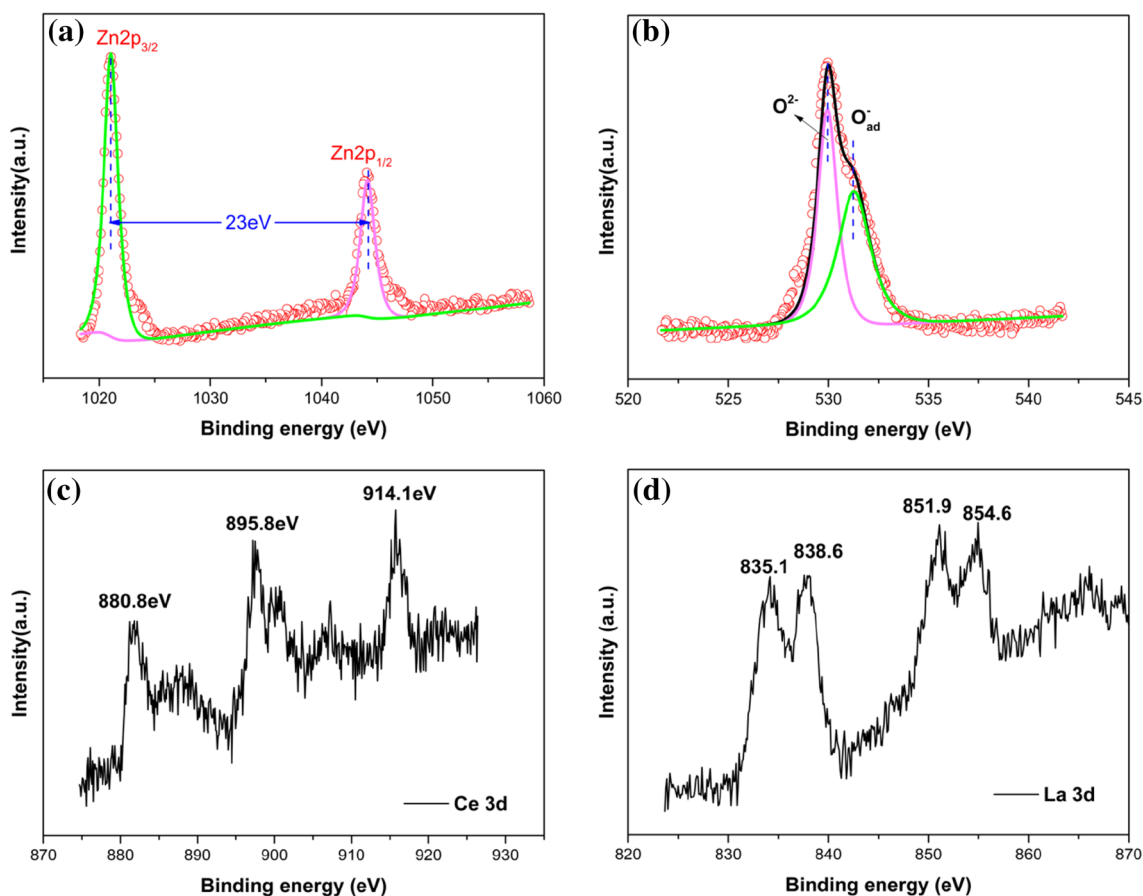


Fig. 4 XPS spectra of the La/Ce-codoped ZnO samples. a Zn p, b O1s, c Ce 3d, d La 3d

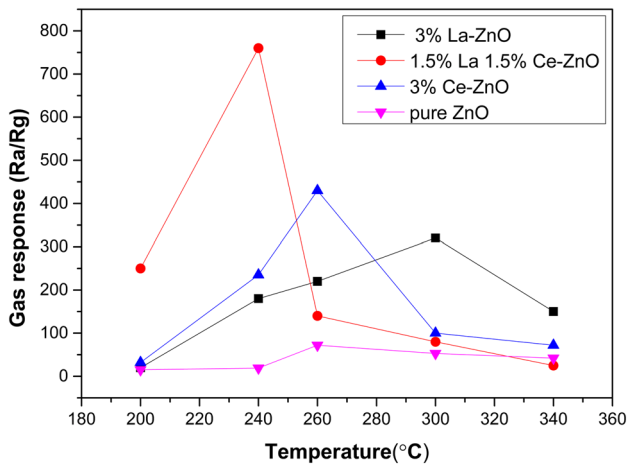


Fig. 5 Responses of ZnO-based sensors to 100 ppm 1,2-propanediol at different operating temperatures

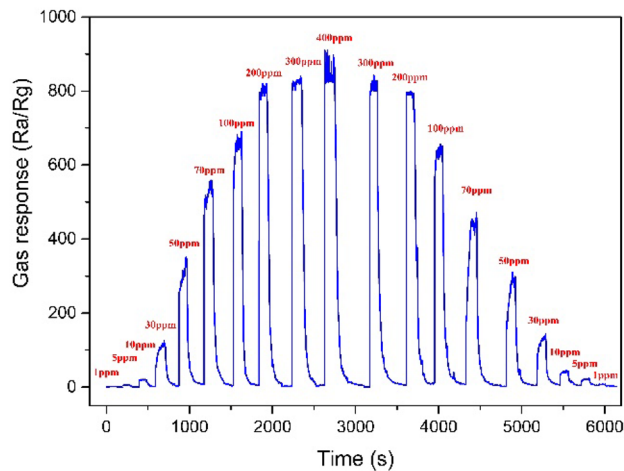


Fig. 6 Dynamic response and recovery curves of La/Ce-co-doped ZnO sensor to different concentrations of 1,2-propanediol at 240 °C

1,2-propanediol at 240 °C. As we can see from Fig. 8a–c, the response time of La-doped ZnO, the La/Ce-codoped ZnO and Ce-doped ZnO is calculated to be 13 s, 11 s and 15 s.

Correspondingly, the recovery time is 106 s, 45 s and 43 s. These data reveal a quicker response and a shorter recovery time of La/Ce-codoped ZnO-based gas sensor than that

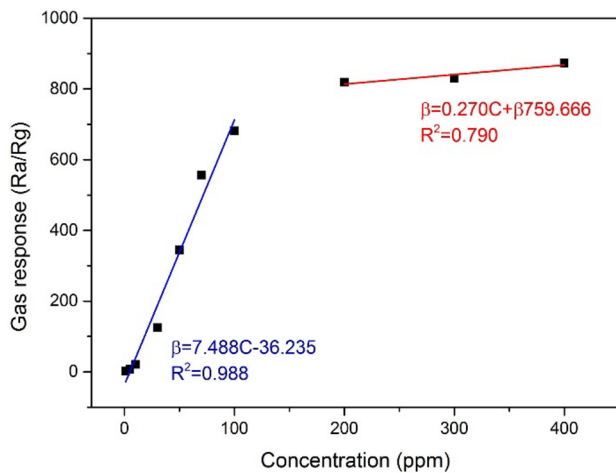


Fig. 7 The corresponding linear relationship between gas response and gas concentration

of singly La-doped ZnO and Ce-doped ZnO, which further proves the better gas-sensing property of La/Ce-codoped ZnO-based gas sensor.

It is well known that the environmental humidity has a great influence on sensitivity. To explore the effect of humidity on the sensitivities of the fabricated 1,2-propanediol gas sensors, we injected the distilled water in the test chamber. The result is shown in Fig. 9. The response–recovery curve of La/Ce-codoped ZnO-based gas sensor is carried out when the gas sensor is exposed to 100 ppm 1,2-propanediol with 250 ppm water vapor (Fig. 9a) or without injected water (Fig. 9b) at 240 °C. The gas sensor performances in above two situations are summarized in Table 2, so it can be deduced that water vapor has no obvious influence on the gas response.

The short-term stability of La/Ce-codoped ZnO-based gas sensor toward 100 ppm 1,2-propanediol at 240 °C is measured, as displayed in Fig. 10a. It is observed that the response of the four adsorption platforms shows a slight variation. The long-term stability of the gas sensor is another significant parameter of the gas sensor. Hence, the long-term

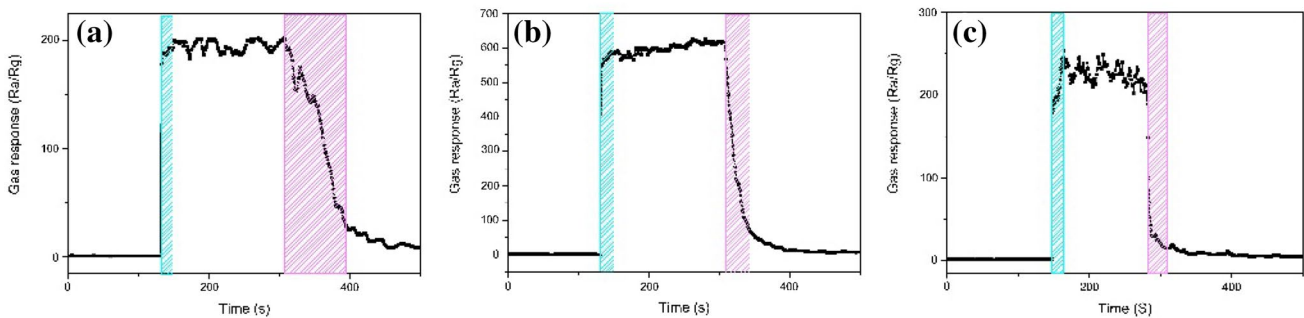


Fig. 8 Response-recovery curve of 3 at.% La-ZnO (a), 1.5 at.% La/1.5 at.% Ce-ZnO (b) and 3 at.% Ce-ZnO (c) to 100 ppm 1,2-propanediol at 240 °C

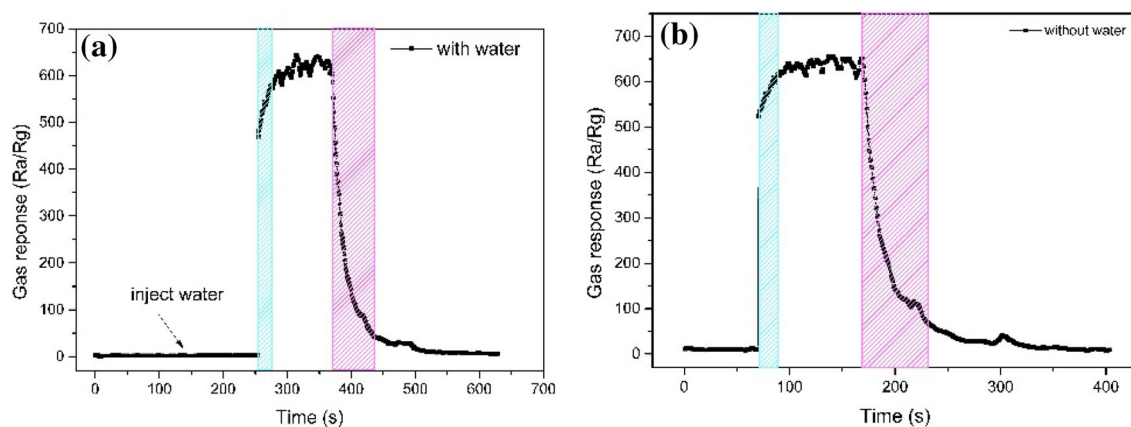


Fig. 9 The response of La/Ce-codoped ZnO change when gas sensor is exposed in 100 ppm 1,2-propanediol and 250 ppm water vapor (a) or not injected water (b)

Table 2 The gas performances of La/Ce-codoped ZnO-based gas sensors change when gas sensor is exposed in 100 ppm 1,2-propanediol and 250 ppm water vapor or not injected water

	Gas response (Ra/Rg)	Response time (s)	Recover time (s)
Inject water	642	19	59
Without water	655	12	52

stability of La/Ce-codoped ZnO is measured. Figure 10b displays the response to 100 ppm 1,2-propanediol at 240 °C as a function of the number of testing days. The sensor response is almost constant even over 20 days. Therefore, La/Ce-codoped ZnO-based gas sensor has both excellent short- and long-term stability.

In addition, to further research the gas selectivity of La/Ce-codoped ZnO, the gas response of La/Ce-codoped ZnO-based gas sensor is tested towards 100 ppm alcohol, 1,2-propanediol, acetone, acetic acid, and formaldehyde at the optimum operating temperature of 240 °C, and the results are shown in Fig. 11. All of the sensors exhibit their maximum gas responses towards 1,2-propanediol. Especially, compared with the other sensors, the La/Ce-codoped ZnO-based gas sensor has superior gas selectivity.

3.3 Gas-sensing mechanism

Gas-sensing mechanism of a typical n-type metal oxide semiconductor such as ZnO is described as the adsorption/desorption process of oxygen on its surface [14]. When the ZnO rod sensor is exposed to ambient air, oxygen species in the air are adsorbed on the ZnO surfaces and capture free electrons from the conduction band of the sensing materials to form O_2^- below 100 °C, or O^- between 100 and 300 °C, or O^{2-} at above 300 °C [15, 16]. Therefore, the adsorbed oxygen species at 240 °C is mainly O_2^- and O^- . At the operating temperature

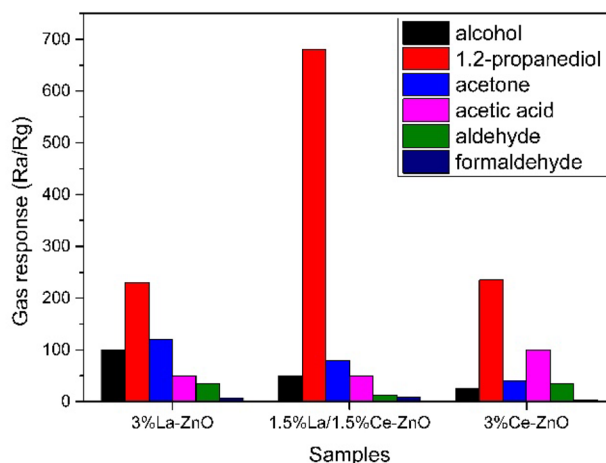


Fig. 11 Selectivity measurements of 3 at.% La-ZnO, 1.5 at.% La/1.5 at.% Ce-ZnO, and 3 at.% Ce-ZnO sensors to various tested gases with concentrations of 100 ppm at 240 °C

lower than 300 °C, the related reactions are expressed as followed formulae [17]:



In the presence of reducing gases, such as 1,2-propanediol, the 1,2-propanediol molecules can react with the former adsorbed oxygen species on the surface of ZnO to form CO_2 and H_2O , and make the trapped electrons release back into the conduction band, thereby decreasing the thickness of the depletion layer and increasing conductivity. Detailed possible reactions with 1,2-propanediol are shown in the following equations:

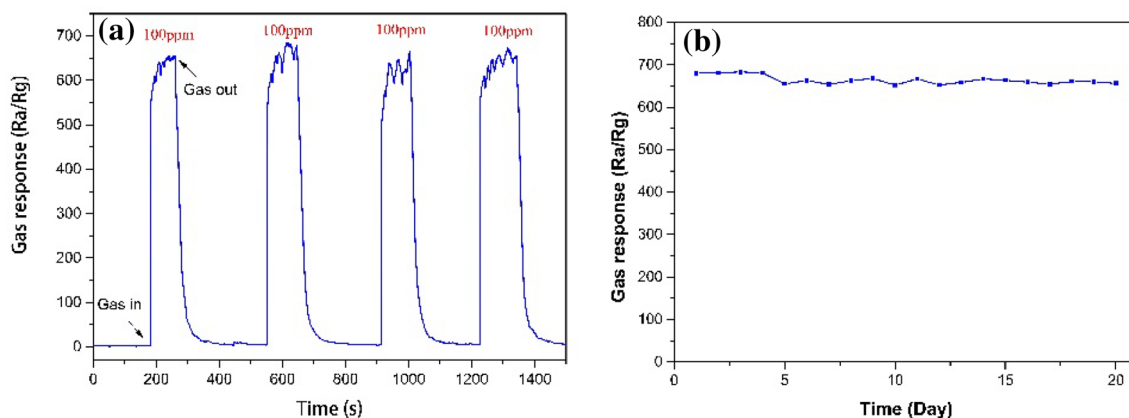
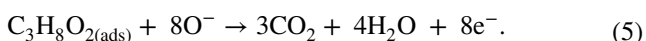


Fig. 10 a Short- and b long-term stability of La/Ce-codoped ZnO-based gas sensor toward 100 ppm 1,2-propanediol at operating temperature of 240 °C



According to the XRD, SEM and EDS analyses, one can find that a bit of La_2O_3 forms on the surface of ZnO rods. In addition, La_2O_3 is reported to be p-type oxides [18]. The p–n heterostructure formed between p-type La_2O_3 and n-type ZnO interfaces plays an important factor in bending the energy band in depletion layer [19]. Then, electrons transfer from n-type ZnO to p-type La_2O_3 while holes transfer contrarily until the Fermi levels of the system are equalized, resulting in a wider depletion layer and the increased initial resistance [2]. Due to the electrical properties of the structural interface, the hetero contact can enhance the 1,2-propanediol adsorption kinetics when La/Ce-co-doped ZnO gas sensor is exposed to 1,2-propanediol gas [20]. At the same time, according to the SEM and XRD analyses, CeO_2 phase congregating on the surface of the ZnO rods plays an important role in dehydrogenation and ring-opening of hydrocarbon [21]. The coarse structure indicates an enhancement in the effective surface area and formation of surface for better adsorption of gas molecules.

Furthermore, owing to the similar relevant ionic radius ($\text{La}^{3+} = 1.160 \text{ \AA}$, $\text{Ce}^{4+} = 0.97 \text{ \AA}$), it seems reasonable for La^{3+} to replace Ce^{4+} partially in the CeO_2 crystallites to form compound of $\text{La}_2\text{O}_3\text{--CeO}_2$. Meantime, trivalent La^{3+} substitutes for Ce^{4+} in the ceria lattice, producing a great number of oxygen vacancies and improving the oxygen storage/release capacity (OS/RC) and the oxygen mobility of ceria. Additionally, La_2O_3 and CeO_2 have good catalytic properties. They can accelerate the dehydrogenate and consecutive oxidation of hydrocarbons, enhancing 1,2-propanediol sensitivity. Therefore, the better gas-sensing properties of La/Ce-codoped ZnO gas sensor are attributed to the synergistic reaction of La_2O_3 and CeO_2 [22].

4 Conclusion

In summary, a facile hydrothermal method is used for the preparation of the La/Ce-codoped ZnO gas sensor. In particular, a comparative gas-sensing investigation clearly demonstrates that the La/Ce-co-doped ZnO gas sensor exhibited a lower optimal operating temperature of 240 °C for 1,2-propanediol gas compared with La-doped ZnO and Ce-doped ZnO gas sensor. In addition, La/Ce-co-doped ZnO gas sensor shows the highest gas response of 681 toward 100 ppm 1,2-propanediol at 240 °C. What's more, it also shows a good response of 2.7 at the low detecting limit of 1 ppm, indicating its good response at low gas concentrations. In the following tests, this gas sensor also exhibits superior selectivity reversibility, repeatability and stability. The possible mechanism may attribute to the formation of $\text{La}_2\text{O}_3\text{--ZnO}$ heterojunction and the synergistic effect of La/Ce-doping.

All these results indicate that the as-synthesized La/Ce-decorated ZnO can be promising materials for its application in 1,2-propanediol detection.

References

1. N.F. Hamedani, A.R. Mahjoub, A.A. khodadadi, Y. Mortazavi, CeO_2 doped ZnO flower-like nanostructure sensor selective to ethanol in presence of CO and CH_4 . *Sens. Actuators B Chem.* **169**, 67–73 (2012)
2. X.L. Xu, Y. Chen, S.Y. Ma, W.Q. Li, Y.Z. Mao, Excellent acetone sensor of La-doped ZnO nanofibers with unique bead-like structures. *Sens. Actuators B Chem.* **213**, 222–233 (2015)
3. F. Gao, G. Qin, Y. Li, Q. Jiang, L. Luo, K. Zhao, Y. Liu, H. Zhao, One-pot synthesis of La-doped SnO_2 layered nanoarrays with an enhanced gas-sensing performance toward acetone. *RSC Adv.* **6**, 10298–10310 (2016)
4. X.F. Chu, X.H. Zhu, Y.P. Dong, X.T. Ge, S.Q. Zhang, W.Q. Sun, Acetone sensors based on La^{3+} doped ZnO nano-rods prepared by solvothermal method. *J. Mater. Sci. Technol.* **28**, 200–204 (2012)
5. H. Xu, A.L. Rosa, T. Frauenheim, R.Q. Zhang, S.T. Lee, Density-functional theory calculations of bare and passivated triangular-shaped ZnO nanowires. *Appl. Phys. Lett.* **91**, 031914 (2007)
6. S.P. Huang, H. Xu, I. Bello, R.Q. Zhang, Tuning electronic structures of ZnO nanowires by surface functionalization a first-principles study. *J. Phys. Chem. C* **114**, 8861–8866 (2010)
7. L.W. Wang, Y.F. Kang, X.H. Liu, S.M. Zhang, W.P. Huang, S.R. Wang, ZnO nanorod gas sensor for ethanol detection. *Sens. Actuators B Chem.* **162**, 237–243 (2012)
8. S.Q. Tian, Y.P. Zhang, D.W. Zeng, H. Wang, N. Li, C.S. Xie, C.X. Pan, X.J. Zhao, Surface doping of La ions into ZnO nanocrystals to lower the optimal working temperature for HCHO sensing properties. *Phys. Chem. Chem. Phys.* **17**, 27437–27445 (2015)
9. S. Tian, Y. Zhang, D. Zeng, H. Wang, N. Li, C. Xie, C. Pan, X. Zhao, Surface doping of La ions into ZnO nanocrystals to lower the optimal working temperature for HCHO sensing properties. *Phys. Chem. Chem. Phys.* **17**, 27437–27445 (2015)
10. X.J. Wang, W. Wang, Y.L. Liu, Enhanced acetone sensing performance of Au nanoparticles functionalized flower-like ZnO. *Sens. Actuators B Chem.* **168**, 39–45 (2012)
11. S.W. Choi, S.S. Kim, Room temperature CO sensing of selectively grown networked ZnO nanowires by Pd nanodot functionalization. *Sens. Actuators B Chem.* **168**, 8–13 (2012)
12. J. Mi, G. Feng, L. Han, T. Guo, Y. Zhu, J. Wang, Modified semi-coke-supported cerium oxide-doped zinc ferrites for the removal of H_2S from coal gas. *Chem. Eng. Technol.* **35**, 1626–1631 (2012)
13. W.R. Lu, D.C. Zhu, X. Xiang, Synthesis and properties of Ce-doped ZnO as a sensor for 1,2-propanediol. *J. Mater. Sci. Mater. Electron.* **28**, 18929–18935 (2017)
14. T. Wang, X. Kou, L. Zhao, P. Sun, C. Liu, Y. Wang, K. Shimano, N. Yamazoe, G. Lu, Flower-like ZnO hollow microspheres loaded with CdO nanoparticles as high performance sensing material for gas sensors. *Sens. Actuators B Chem.* **250**, 692–702 (2017)
15. N.S. Ramgir, P.K. Sharma, N. Datta, M. Kaur, A.K. Debnath, D.K. Aswal, S.K. Gupta, Room temperature H_2S sensor based on Au modified ZnO nanowires. *Sens. Actuators B Chem.* **186**, 718–726 (2013)
16. K. Shingange, Z.P. Tshabalala, O.M. Ntwaeaborwa, D.E. Motung, G.H. Mhlongo, Highly selective NH_3 gas sensor based on Au loaded ZnO nanostructures prepared using microwave-assisted method. *J. Colloid Interface Sci.* **479**, 127–138 (2016)
17. X. Xiang, D. Zhu, D. Wang, Enhanced formaldehyde gas sensing properties of La-doped SnO_2 nanoparticles prepared by

- ball-milling solid chemical reaction method. *J. Mater. Sci. Mater. Electron.* **27**, 7425–7432 (2016)
18. A.A. Yadav, A.C. Lokhande, P.A. Shinde, J.H. Kim, C.D. Lokhande, CO₂ gas sensing properties of La₂O₃ thin films deposited at various substrate temperatures. *J. Mater. Sci. Mater. Electron.* **28**, 13112–13119 (2017)
 19. H.-J. Kim, J.-H. Lee, Highly sensitive and selective gas sensors using p-type oxide semiconductors: overview. *Sens. Actuators B Chem.* **192**, 607–627 (2014)
 20. S. Aygun, D. Cann, Response kinetics of doped CuO/ZnO hetero-contacts. *J. Phys. Chem. B* **109**, 7878–7882 (2005)
 21. C. Ge, C. Xie, S. Cai, Preparation and gas-sensing properties of Ce-doped ZnO thin-film sensors by dip-coating. *Mater. Sci. Eng. B* **137**, 53–58 (2007)
 22. C.S. Yang, J.H. Chen, S.J. Dai, Application of ceria and lanthana in catalyst for cleansing exhaust gas of car. *J. Rare Earth* **22**, 232–235 (2004)